Proceedings of the 7th GACM Colloquium on Computational Mechanics
for Young Scientists from Academia and Industry
October 11-13, 2017 in Stuttgart, Germany

Kriging-guided Level Set Method for Crash Topology Optimization

Elena Raponi[1]*, Mariusz Bujny[2], Markus Olhofer[3], Nikola Aulig[3], Simonetta Boria[1] and Fabian Duddeck[2]

Micro Abstract
Crashworthiness optimization problems are characterized by strong nonlinearities and discontinuities. Hence, gradient-based methods cannot be used and alternative approaches have to be considered. Here, a novel, kriging-based method for level set topology optimization is proposed and validated on a crash test case. Compared to CMA-ES, this method demonstrates to be efficient in terms of convergence speed and promising in the context of crash topology optimization.

[1]Mathematics and Applications, University of Camerino, Camerino, Italy
[2]Chair of Computational Mechanics, Technical University of Munich, München, Germany
[3]Complex System Optimization and Analysis, Honda Research Institute Europe GmbH, Offenbach am Main, Germany
***Corresponding author**: elena.raponi@studenti.unicam.it

Introduction

Structural Topology Optimization (TO) [5] was first introduced by Bendsøe and Kikuchi [4]. It is a well-developed discipline which aims to determine constructive solutions for component structures through changing material distribution in a given design space so as to obtain an optimal performance of the concept design. Since crashworthiness optimization problems are characterized by high nonlinearities, noisiness and discontinuities of the objective functions to be optimized, heuristics are frequently introduced in TO strategies, which are often not accepted by the engineering community. As such, alternative approaches to the most known TO methods (Equivalent Static Loads methods [12,22,28], Ground Structure Approaches [17,29], Bubble and Graph/Heuristic-based approaches [13,14,26], Hybrid Cellular Automata techniques [25,30]) have to be found. Recently, a novel approach for optimization of crash problems, the Evolutionary Level Set Method (EA-LSM) for crash Topology Optimization, was proposed [7–9]. This approach uses Evolutionary Algorithms (EAs) [3] to handle the update process when no reliable gradient information can be used. However, Evolution Strategies require thousands of calls to the high-fidelity analysis codes to locate a near optimal solution. Therefore, they are substituted in this work by an optimization strategy introducing Surrogate Modeling techniques [16]. They replace the direct optimization of the computationally expensive model by an iterative process that consists of the creation, optimization and updating of a surrogate model that, being orders of magnitude cheaper to run, can be used to obtain many more evaluations during the optimization process. The key component of any surrogate-based optimization algorithm is the approximation model, which can be chosen among a multitude of alternatives: Polynomial Regression [11,16], Radial Basis Function [6,16], Kriging [2,16,23], Support Vector Regression [18,34], Artificial Neural Networks [24,35] and others. The results of this research were obtained by using a Kriging-guided Level Set Topology Optimization Method (KG-LSM) [32], which couples the Level Set Method with a Kriging-surrogate approximation model. The choice of the Kriging surrogate is motivated by several reasons. Firstly, the high accuracy of the model was confirmed by carrying out some testing on the different surrogates. In addition, relevant flexibility is given by the parameters' estimation at each iteration of the approximating algorithm. Finally, the model is able to furnish an estimate of the potential error in the approximation, useful in a crucial phase of the optimization procedure, described later. The state-of-the-art Covariance Matrix Adaptation Evolution Strategy (CMA-ES) [20] is taken as a reference to compare the convergence properties and the optimized designs resulting from the proposed approach.

The paper has the following structure. Section 1 describes the adopted optimization strategy, characterized by an implicit parametrization with geometric level set functions and a Kriging-guided updating process. Moreover, the considered optimization problem and the techniques to handle constraints are presented. In Section 2, the experimental test case and the obtained results are discussed. Final conclusions are drawn at the end.

1 Optimization strategy

1.1 Level Set Method Parametrization

The great majority of structural TO methods belong to the group of density-based approaches [1]. An alternative to these strategies is given by the Level Set Method. In the level set framework [27], the material distribution is given by a boundary defined by a *level set* (*iso-contour*) of an embedding scalar function: the *Level Set Function* (LSF). During the optimization problem, the structural boundaries move due to the changes in the embedding function. As a result, interior and exterior boundaries may merge with each other, new holes may be created or preexisting ones deleted. All the TO approaches share three base key concepts: the LSF parametrization, the mechanical model and the optimization strategy.

The LSF parametrization used in this work is inspired by the definitions by Guo et al. [19] and Bujny et al. [7]. The global LSF is defined in order to assume positive values inside the domain areas occupied by material Ω, negative values outside ($D \backslash \Omega$) and to be equal to 0 on the boundary $\partial\Omega$. It is composed by local basis functions, representing many elementary beam components free to move and overlap on the design domain:

$$\phi_i(\mathbf{x}) = -\left[\left(\frac{\cos\theta_i(x-x_{0i})+\sin\theta_i(y-y_{0i})}{l_i/2}\right)^m + \left(\frac{-\sin\theta_i(x-x_{0i})+\cos\theta_i(y-y_{0i})}{t_i/2}\right)^m - 1\right], \quad (1)$$

where $\mathbf{x} = (x, y)^T$ is a point of the bidimensional domain $D = \mathbb{R}^2$ and (x_0, y_0) denotes the position of the centre of the component with length l, thickness t, and rotation angle θ, as shown in Fig. 1(a). m is a relatively large even integer number, usually taken equal to 6 [7, 19]. The

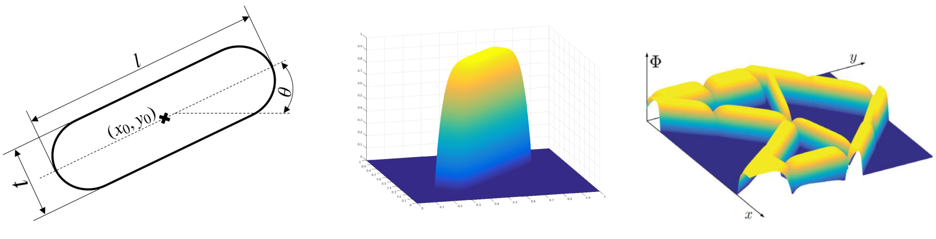

(a) (b) (c)

Figure 1. Structural components details [7]: (a) component parametrization, (b) corresponding local level set function, where negative values are set to zero, (c) combination of local level set functions.

LSF is then mapped to the finite element mesh through a density-based geometry mapping [7, 32] and an optimization strategy by means of Kriging-guided mathematical programming is carried out, whose basics are presented in the following section.

1.2 Kriging Optimization Algorithm

The update procedure proposed in this work is the Efficient Global Optimization (EGO) algorithm [2, 21]. The algorithm starts with a Design of Experiments (DoE) [10], which allows for sampling the high-fidelity function uniformly within the considered domain, and then constructs a model to approximate the expensive function. Based on the latter, new points (*infill points*) are chosen and added one at each iteration to the initial DoE samples, in order to improve the quality of the approximation. In this research, a Kriging surrogate model starting from an Optimal Latin Hypercube Sampling (OHLS) [15] was used and updated iteratively with the use of Differential Evolution (DE) [33] by maximizing proposed variants of the standard Expected Improvement (EI) infill criterion [16].

The DoE training data are seen as results of a stochastic process and denoted by using a set of random vectors $\mathbf{Y}(\mathbf{x}) = [Y(\mathbf{x}^{(1)}), ..., Y(\mathbf{x}^{(n)})]^T$, with mean $\mathbf{1}\mu$, where $\mathbf{1}$ is an n x 1 column vector of ones. Moreover, the correlation between each couple of random variables is described using a squared-exponential basis function expression:

$$\psi(\mathbf{x}^{(i)}, \mathbf{x}^{(l)}) \equiv cor[Y(\mathbf{x}^{(i)}), Y(\mathbf{x}^{(l)})] = e^{-\sum_{j=1}^{k} \theta_j |x_j^{(i)} - x_j^{(l)}|^2}, \tag{2}$$

where the $\boldsymbol{\theta}$ vector allows the width of the basis function to differ from variable to variable and can be estimated by using the likelihood of the predicted data $\mathbf{y}$, defined as:

$$L(Y^{(1)}, ..., Y^{(n)} | \mu, \sigma) = \frac{1}{(2\pi\sigma^2)^{n/2}} e^{-\frac{\sum (Y^{(i)} - \mu)^2}{2\sigma^2}}. \tag{3}$$

After appropriate substitutions and simplifications, the natural logarithm of Eq. (3) is considered. By deriving and setting the derivative to zero, the maximum likelihood estimates (MLEs) for the mean μ and variance σ^2 are obtained and used to predict the model response $\hat{y}$ at a new location $\mathbf{x}$ and the committed error in the prediction $\hat{s}^2$ [16, 32]:

$$\hat{y}(\mathbf{x}) = \hat{\mu} + \boldsymbol{\psi}^T \boldsymbol{\Psi}^{-1} (\mathbf{y} - \mathbf{1}\hat{\mu}), \qquad \hat{s}^2(\mathbf{x}) = \hat{\sigma}^2 \left[1 - \boldsymbol{\psi}^T \boldsymbol{\Psi}^{-1} \boldsymbol{\psi} + \frac{1 - \mathbf{1}^T \boldsymbol{\Psi}^{-1} \boldsymbol{\psi}}{\mathbf{1} \boldsymbol{\Psi}^{-1} \mathbf{1}} \right], \tag{4}$$

where $\boldsymbol{\Psi}$ is the correlation matrix between the random variables.

The estimation of the uncertainty on the interpolated function value is essential to define the EI updating criterion:

$$E[I(\mathbf{x})] = \begin{cases} (y_{min} - \hat{y}(\mathbf{x}))\Phi\left(\frac{y_{min} - \hat{y}(\mathbf{x})}{\hat{s}(\mathbf{x})}\right) + \hat{s}(\mathbf{x})\phi\left(\frac{y_{min} - \hat{y}(\mathbf{x})}{\hat{s}(\mathbf{x})}\right) & \text{if } \hat{s}(\mathbf{x}) > 0 \\ 0 & \text{if } \hat{s}(\mathbf{x}) = 0 \end{cases} \tag{5}$$

where Φ and ϕ are the Gaussian cumulative distribution function and probability density function respectively. One major advantage of Eq. (5) is that it allows to locate new points in both promising areas, close to the best values observed so far, and the less explored ones, characterized by a low sampling density.

1.3 Optimization Problem and Constraint Handling

In this work, an optimization problem of the following form is dealt with:

$$\begin{aligned} \min_{\mathbf{x}} \quad & f_{obj}(\mathbf{x}), \\ \text{s.t.} \quad & r(t) = 0, \\ & g_i(\mathbf{x}) \leq 0, \qquad i = 1, ..., m, \quad \mathbf{x} \in \mathbb{R}^n, \end{aligned} \tag{6}$$

where f_{obj} is the objective function to be minimized, $r(t) = 0$ is the condition which expresses the dynamic equilibrium at time t and g_i, $i = 1, ..., m$, are the inequality constraints. The vector $\mathbf{x}$ of the design variables collects all the parameters defining the LSM basis functions. In this work, the objective function f_{obj} is the intrusion of an impacting pole in a transverse bending crash scenario, where the structure is subjected to a connectivity and a volume constraint. The first aims to ensure that the designs obtained during the optimization process make physical sense, while the second is necessary to meet the industrial requirements of limited mass for each designed component. Different techniques to handle the constraints were developed.

The Expected Improvement for Connected Designs (EICD) is a proposed variant of the standard EI that ensures the connectivity of the promising candidates in the infill procedure. When disconnected designs are met during the maximization of EI by DE, a penalty which is proportional to the level of infeasibility is computed:

$$P = \gamma(P_{S1} + P_{S2} + P_C), \tag{7}$$

where P_{S1} and P_{S2} are the minimum distances between the structure and the left-hand side and right-hand side supports respectively. In case the design is split in disconnected parts, P_C is the minimum distance between those sub-structures and γ is a suitable penalty factor. A graphical representation of the penalty distances is given in Fig. 2.

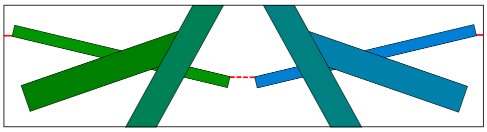

Figure 2. Example of violation of the connectivity constraint. The red solid lines represent the extra-distances between the structure and the supports, which are equivalent due to the symmetry condition. The red dashed line indicates the minimum distance between different connected components.

The penalty P is used to modify Eq. (5) as follows:

$$E[I(\mathbf{x})] = \begin{cases} E[I(\mathbf{x})] & \text{if } \mathbf{x} \text{ is connected,} \\ -P(\mathbf{x}) & \text{if } \mathbf{x} \text{ is disconnected.} \end{cases} \tag{8}$$

As a result, the disconnected designs are automatically discarded in the maximization of Eq. (8).

The Constrained Expected Improvement (CEI) [16] is used to drive the infill search towards designs which do not exceed the admitted volume limit (set to the 50% of the entire area of the design domain). It maximizes the product between EI and the Probability of Feasibility (PF), i.e. the probability that the volume constraint is satisfied:

$$\mathbf{x}_{infill} = \underset{\mathbf{x}}{\text{argmax}} \;\; E[I(\mathbf{x})]P[F(\mathbf{x})]. \tag{9}$$

An alternative to the CEI is the exterior penalty method [31], whose ability to guarantee the volume requirements is tested in this work for both the proposed Kriging-guided optimization algorithm and the CMA-ES.

2 Test case and results

The considered dynamic test is performed on a standard transverse bending case, where a cylindrical pole impacts in the middle of a structure defined on a rectangular design domain, fixed at both ends (Fig. 3(a)). The optimization goal is to minimize the intrusion of the pole into the structure. The level set function is mapped on the reference LS-Dyna mesh, shown in Fig 3(b). It is composed of 1600 eight-node solid elements, which are assigned a piecewise linear plasticity material. The test settings are shown in Table 1.

This work presents a 6-beams 15-variables problem to evaluate the KG-LSM performance in a constrained dynamic environment. Despite the low number of parameters, reasonably good structures can be obtained thanks to the used parametrization. Indeed, a reference configuration of 6 beams arranged within the design domain according to Fig. 4 is considered. A symmetry of the design with respect to the domain vertical symmetry axis is assumed and all the beams' parameters are allowed to change during the optimization process. Starting from a 200-samples DoE, the following strategies have been compared (Fig. 5):

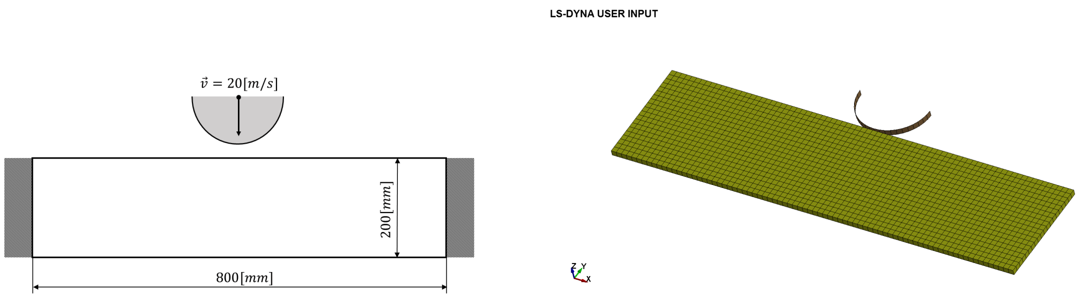

(a) (b)

Figure 3. Transverse Bending test case: (a) problem definition and (b) LS-Dyna FEM mesh.

Property	Symbol	Value	Unit
Beam material density	ρ	$2.7 \cdot 10^3$	kg/m^3
Young's modulus	E	$7.0 \cdot 10^4$	MPa
Poisson's ratio	ν	0.33	-
Yield stress	R_e	241.0	MPa
Tangent modulus	E_{tan}	70.0	MPa
Pole velocity	v	20	m/s
Pole mass	m	11.815	kg
Pole diameter	D	139.154	mm

Table 1. Configuration of the considered transverse bending test case.

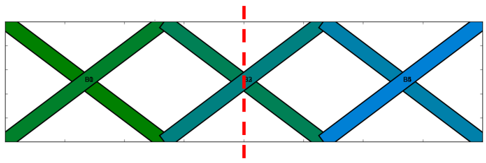

Figure 4. Reference 6-beams configuration for the dynamic transverse bending test case.

- CMA-ES: Covariance Matrix Adaptation Evolution Strategy initialized with the 6-beams reference structure in Fig. 4 and volume constrain handled by the exterior penalty method;
- DoE-CMA-ES: Covariance Matrix Adaptation Evolution Strategy initialized with the best design resulting from the DoE phase and volume constrain handled by the exterior penalty method;
- KG-LSM-DoEsel-EICD-CEI: Kriging-guided optimization method with initial DoE selection by removing the infeasible points and the EICD coupled with CEI infill criterion to handle both the connectivity and the volume constraint during the infill procedure;
- KG-LSM-DoEvar-EICD-volpenalty: Kriging-guided optimization method with initial DoE selection by removing the infeasible points and the EICD coupled with an exterior penalty method to handle both the connectivity and the volume constraint during the infill procedure.

For both CMA-ES and DoE-CMA-ES, a population size of 6 parent and 12 offspring individuals is considered. In the third tested configuration, the coupling between EICD and CEI is obtained by applying the connectivity check described in Section 1.3 in the maximization of the EI·PF.

In Figure 5(a), the superiority of the Kriging-guided methods is evident throughout the optimization process. Not only the convergence is faster at the beginning, but also CMA-ES strategies are not able to reach the average performance of KG-LSM methods within the considered range of evaluations. It is worth noting that both the KG-LSM methods outperform DoE-CMA-ES, which is initialized by choosing the first population of parent individuals as the

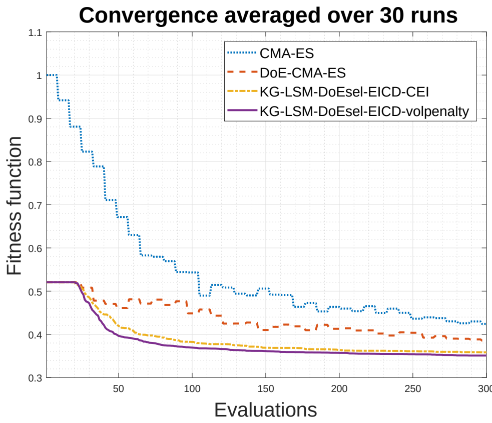

(a)

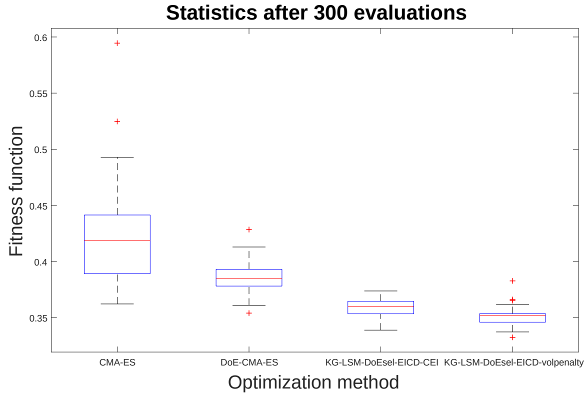

(b)

Figure 5. Comparison of the optimizations' average convergence over 30 runs of the proposed KG-LSM methods and CMA-ES for the 15-variables transverse bending test case (a) box plot after 300 evaluations (b). The initial flat trends in (a) are obtained by replicating the best DoE fitness value for the number of performed evaluations in the DoE phase.

best DoE sample, available from the surrogate-based procedure. Therefore, the good convergence properties of the proposed optimization approach do not exclusively depend on the initial DoE procedure. The intrinsic nature of the EICD infill criterion, balancing exploitation and exploration, leads to a more efficient search than the DoE-CMA-ES one, which shows a more exploitive behavior and converges frequently to local optima.

The boxplot in Figure 5(b) confirms the lower optimum values of the Kriging-guided strategies. After 300 evaluations, the statistics among 30 runs illustrate a quite uniform behavior of the KG-LSM methods, KG-LSM-DoEsel-EICD-volpenalty in particular. In fact, they show a smaller variance value with respect to the two considered Evolution Strategies.

When it comes to the obtained topologies, even more interesting results can be observed. Fig. 6 shows the best designs obtained by the DoE-CMA-ES and the Kriging-guided optimization strategies, compared to the best and the second best optimum available from a research by Bujny et al. [9], where the same test case is studied. It has to be noted that the designs resulting from

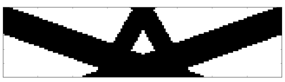

(a)

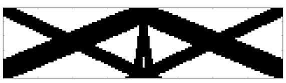

(b)

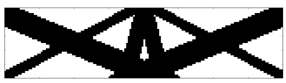

(c)

(d)

(e)

Figure 6. Best designs for the intrusion minimization problem obtained with (a) DoE-CMA-ES, (b) KG-LSM-DoEsel-EICD-CEI and (c) KG-LSM-DoEsel-EICD-volpenalty compared to the best (d) and second best (e) optimal layouts available in the literature [9] for the same test case.

the KG-LSM strategies (Fig. 6(b)-6(c)) are not only qualitatively superior to the best layout from DoE-CMA-ES, shown in Fig. 6(a), but also fully consistent with the ones available in the literature [9] (Fig. 6(d)-6(e)). In particular, the KG-LSM-DoEsel-EICD-CEI is able to find the local optimum shown in Fig. 6(e) with a much lower computational effort than needed to reach the optimum by using Evolution Strategies. Therefore, very good results were obtained from both the convergence and the final designs point of view. This represents a significant evidence of the proposed method's capabilities in providing useful indications for the practical construction of structural components and a sufficient reason to go for further investigations.

Conclusions

In this work, a novel KG-LSM was presented and used for identification of optimal topologies of beam structures in a transverse bending test problem. Different techniques to handle two types of constraints - connectivity and volume - were applied. The convergence behavior and the final material distributions were presented to analyze the performance of the proposed Kriging-guided Topology Optimization strategy in a crashworthiness context, where the applicability of the standard crashworthiness optimization methods is limited due to the strong nonlinearities and discontinuities characterizing the problem.

Every KG-LSM strategy was compared with the state-of-the-art CMA-ES in a pole intrusion minimization problem. A DoE-CMA-ES strategy was also used for comparison purposes, due to the high influence the DoE procedure has on the optimization process itself. Fast convergence capabilities and a good performance of the obtained designs were found, confirming the method to be promising in the context of crash topology optimization. In fact, since many expensive optimization problems, such as crashworthiness ones, are limited by the available number of iterations, a fast convergence at the initial stages of the optimization process is often desired. The high-quality beam topologies are an ulterior evidence of the KG-LSM ability to identify optimal concept designs in early stages of the product development process. Moreover, since no sensitivity information is needed to carry out the optimization process, the proposed method offers great flexibility in many applications. The promising results motivate future analyzes on higher-dimensional crash problems and alternative objective functions.

References

[1] G. Allaire, F. Jouve, and A. M. Toader. Structural optimization using sensitivity analysis and a level-set method. *Journal of Computational Physics*, 194(1):363–393, 2004.

[2] I. Arsenyev. *Efficient Surrogate-based Robust Design Optimization Method.* PhD thesis, Technische Universität München, 2017.

[3] T. Bäck and H. P. Schwefel. An Overview of Evolutionary Algorithms for Parameter Optimization. *Evolutionary Computation*, 1(1):1–23, 1993.

[4] M. P. Bendsøe and N. Kikuchi. Generating optimal topologies in structural design using a homogenization method. *Computer Methods in Applied Mechanics and Engineering*, 71(2):197–224, 1988.

[5] M. P. Bendsøe and O. Sigmund. *Topology Optimization - Theory, Methods, and Applications.* Springer, second edition, 2004.

[6] D. S. Broomhead. *Radial Basis Functions, Multi-variable Functional Interpolation and Adaptive Networks.* Royals Signals & Radar Establishment, 1988.

[7] M. Bujny. Development of a Hybrid Evolutionary Approach for Level Set Topology Optimization. Master's thesis, Technische Universität München, 2015.

[8] M. Bujny, N. Aulig, M. Olhofer, and F. Duddeck. Evolutionary Level Set Method for Crashworthiness Topology Optimization. In *VII European Congress on Computational Methods in Applied Sciences and Engineering*, 2016.

[9] M. Bujny, N. Aulig, M. Olhofer, and F. Duddeck. Identification of optimal topologies for crashworthiness with the evolutionary level set method. *International Journal of Crashworthiness*, 2017. DOI: 10.1080/13588265.2017.1331493.

[10] M. Cavazzuti, A. Baldini, E. Bertocchi, D. Costi, E. Torricelli, and P. Moruzzi. High performance automotive chassis design: a topology optimization based approach. *Structural and Multidisciplinary Optimization*, 44(1):45–56, 2011.

[11] A. Conn, K. Scheinberg, and L. Vicente. *Introduction to Derivative-Free Optimization*. MOS-SIAM Series on Optimization. Society for Industrial and Applied Mathematics, 2009. DOI: 10.1137/1.9780898718768.

[12] F. Duddeck and K. Volz. A new Topology Optimization Approach for Crashworthiness of Passenger Vehicles Based on Physically Defined Equivalent Static Loads. In *ICrash International Crashworthiness Conferemce*, 2012.

[13] H. A. Eschenauer, V. V. Kobelev, and A. Schumacher. Bubble method for topology and shape optimization of structures. *Structural optimization*, 8(1):42–51, 1994.

[14] H. A. Eschenauer and A. Schumacher. Topology and Shape Optimization Procedures Using Hole Positioning Criteria. In *Topology Optimization in Structural Mechanics*, number 374 in International Centre for Mechanical Sciences, pages 135–196. Springer Vienna, 1997.

[15] K. T. Fang, R. Li, and A. Sudjianto. *Design and Modeling for Computer Experiments*. CRC Press, 2005.

[16] A. I. J. Forrester, A. Sóbester, and A. J. Keane. *Engineering Design via Surrogate Modelling - A Practical Guide*. John Wiley & Sons Ltd., 2008.

[17] H. Fredricson, T. Johansen, A. Klarbring, and J. Petersson. Topology optimization of frame structures with flexible joints. *Structural and Multidisciplinary Optimization*, 25(3):199–214, 2003.

[18] S. R. Gunn. *Support Vector Machines for Classification and Regression*. 1998. Technical Report.

[19] X. Guo, W. Zhang, and W. Zhong. Doing Topology Optimization Explicitly and Geometrically - A New Moving Morphable Components Based Framework. *Journal of Applied Mechanics*, 81(8):081009, 2014.

[20] N. Hansen, S. D. Müller, and P. Koumoutsakos. Reducing the Time Complexity of the Derandomized Evolution Strategy with Covariance Matrix Adaptation (CMA-ES). *Evolutionary Computation*, 11(1):1–18, 2003.

[21] D. R. Jones, M. Schonlau, and W. J. Welch. Efficient Global Optimization of Expensive Black-Box Functions. *Journal of Global Optimization*, 13(4):455–492, 1998.

[22] B. S. Kang, W. S. Choi, and G. J. Park. Structural optimization under equivalent static loads transformed from dynamic loads based on displacement. *Computers & Structures*, 79(2):145–154, 2001.

[23] J. P. C. Kleijnen. Kriging metamodeling in simulation: A review. *European Journal of Operational Research*, 192(3):707–716, 2009.

[24] D. Kriesel. *A Brief Introduction to Neural Networks*. 2007.

[25] C. Mozumder, J. E. Renaud, and A. Tovar. Topometry optimisation for crashworthiness design using hybrid cellular automata. *International Journal of Vehicle Design*, 60(1-2), 2012.

[26] C. Ortmann and A. Schumacher. Graph and Heuristic Based Topology Optimization of Crash Loaded Structures. *Structural and Multidisciplinary Optimization*, 47(6):839–854, 2013.

[27] S. Osher and R. P. Fedkiw. Level Set Methods: An Overview and Some Recent Results. *Journal of Computational Physics*, 169(2):463–502, 2001.

[28] G. J. Park. Equivalent Static Loads Method for Non Linear Static Response Structural Optimization. In *LS-DYNA Forum*, Bamberg, 2010.

[29] C. B. W. Pedersen. Topology optimization design of crushed 2d-frames for desired energy absorption history. *Structural and Multidisciplinary Optimization*, 25(5-6):368–382, 2003.

[30] C. L. Penninger, L. T. Watson, A. Tovar, and J. E. Renaud. Convergence analysis of hybrid cellular automata for topology optimization. *Structural and Multidisciplinary Optimization*, 40(1-6):271–282, 2010.

[31] S. S. Rao. *Engineering Optimization: Theory and Practice*. John Wiley & Sons, 1996.

[32] E. Raponi. Development of Surogate Modeling Techniques for Level Set Topology Optimization. Master's thesis, University of Camerino, 2017.

[33] R. Storn and K. Price. Differential Evolution – A Simple and Efficient Heuristic for global Optimization over Continuous Spaces. *Journal of Global Optimization*, 11(4):341–359, Dec. 1997.

[34] V. N. Vapnik. *The Nature of Statistical Learning Theory*. Springer-Verlag New York, Inc., New York, USA, 1995.

[35] J. Zurada. *Introduction to Artificial Neural Systems*. West Publishing Company, St. Paul, MN, USA, 1992.